BRILL

JOURNAL OF CRUSTACEAN BIOLOGY, 33(6), 818-827, 2013

Journal of Crustacean Biology

MOTOR NERVE TERMINAL MORPHOLOGY WITH UNLOADING AND RELOADING OF MUSCLE IN *PROCAMBARUS CLARKII*

Ann S. Cooper [1], Andrew F. M. Johnstone [2,*], and Robin L. Cooper [2,**]

[1] Division of Physical Therapy, Department of Rehabilitation Sciences, College Health Sciences, University of Kentucky, 900 S. Limestone, CTW204L, Lexington, KY 40536-0200, USA

[2] Department of Biology, Center for Muscle Biology, University of Kentucky, 675 Rose Street, Lexington, KY, USA

ABSTRACT

Skeletal muscle shows dynamic changes in mass that correlate with activity and weight bearing loads. The electrical excitation of the muscle of *Procambarus clarkii* (Girard, 1952) used in this study is graded which requires refined nerve-muscle matching in synaptic efficacy. We used the anterior levator (a.l.) muscle in crayfish as a model to address matching of the extent of nerve terminal and muscle size. This muscle repetitively becomes loaded and unloaded for various lengths of time due to limb autotomy. When an adult *P. clarkii* loses a cheliped, by autotomy, the a.l. muscle will atrophy over time. The leg stump still moves suggesting functional innervation. During atrophy, the muscle is drastically reduced in mass as compared to the contralateral control with a functional intact cheliped. The a.l. muscle is innervated by multiple excitatory neurons and at least 1 inhibitory neuron. Since the innervation is less extensive and identifiable for the inhibitory neuron the focus was on the innervation profile based on anti-GABA immunocytochemistry. Preliminary findings based on electron microscopic images of a few samples suggest that terminals on atrophied muscles have fewer synapses than terminals on control muscles. In addition, the extent of terminals on atrophied muscle is much more extensive as compared to muscle per surface area for animals with intact chelipeds. The atrophied muscles appear to be hyperinnervated when considering terminal length per surface area of muscle fiber.

KEY WORDS: crayfish, muscle, neuromuscular junction, plasticity, *Procambarus clarkii*

DOI: 10.1163/1937240X-00002187

INTRODUCTION

How synapses form throughout development and are maintained are key questions in understanding the function of the nervous system. This topic is being addressed by approaches using genetics (Goldstein et al., 2012), to whole brain imaging (Owen et al., 2012) across various animal models and types of synapses (Pacifici et al., 2011; Turner et al., 2011). Investigating synaptic connections at identifiable cells, such as at the neuromuscular junction (NMJ), provides details that are difficult to examine within the central nervous system due to the complexity and accessibility. Examining identifiable terminals at NMJs allows one to readily obtain gross morphometrics as well as addressing ultrastructure of the terminal. The NMJ has proven to be very advantageous over the years in understanding synaptogenesis, plasticity, and maintenance of synaptic structure and function (Grinnell, 1995; Sanes and Lichtman, 1999) which has been applicable for many types of synapses.

The physiological studies of synaptic communication at NMJs provided the basis for the quantal hypothesis of transmission for all chemical synapses (Fatt and Katz, 1953a; Del Castillo and Katz, 1954). Besides development and maintenance issues, NMJs allow one to examine the regression of synapses and reformation that are not as readily studied in an intact CNS. Activity dependence of motor neurons share analogous principles of synaptic development and maintenance with central synapses (Hubel and Wiesel, 1970; Marques, 2005). It is of interest in both the CNS, as well as at the NMJ, to examine how a target influences the presynaptic terminals in development and establish connections which remain semi-stable (Balice-Gordon et al., 1990; Lomo, 2003). Graded synaptic responses of the crayfish NMJ require fine regulation in synaptic transmission for producing coordinated muscle contraction as compared to mammalian muscles, since exceeding a threshold induces an action potential for most mammalian skeletal muscles. The use of NMJs in crustaceans set the stage for many future investigations in synaptic physiology (Fatt and Katz, 1953a, b; Cooper and Cooper, 2009). Unloading of musculature in crustaceans (Velez et al., 1981) and mammals results in muscle mass regression which can also be induced with reducing postsynaptic activity (Edgerton and Roy, 1994; Talmadge, 2000; Deschenes et al., 2003). In addition, unloading a muscle is a means to experimentally simulate weightlessness (Ohira, 2000; Kawano, 2004), which is of interest in addressing environmental conditions of space on motor units and skeletal muscle function. There are numerous topics to be addressed in the cellular responses that result in a functioning

* Current address: United States Environmental Protection Agency, Office of Research and Development, Toxicity Assessment Division, Neurotoxicology Branch, RTP, NC 27711, USA.

** Corresponding author; e-mail: RLCOOP1@email.uky.edu

muscle fiber to degenerate with disuse or unloading while continuing to physiologically function (Reid, 2001, 2005; Herrera and Zeng, 2003). The electrical properties of the plasma membrane also need to be regulated with muscle fiber growth or atrophy in order to allow the muscle to remain functional during the dynamic changes in force of contraction and ionic balance. The interest of this study is addressing motor nerve terminal morphology in a unloaded and reloaded muscle. The synaptic homeostasis at crayfish NMJs, particularly for these graded synaptic connections, is of interest as a potential model in post- and pre-synaptic communication for future mechanistic studies (Cooper et al., 1995; Mykles et al., 2002).

The experimental use in crayfish muscle is of interest due to most fibers being non-spiking and having few motor neurons, one-to-several, which innervate any given skeletal muscle (Atwood, 1973). In addition, the inhibitory motor neuron of the anterior levator (a.l.) muscle can be selectively stained by immunocytochemistry for GABA (Griffis et al., 2001). The crayfish, *Procambarus clarkii* (Girard, 1952), is bilaterally symmetric in the chelipeds so contralateral muscles can be used as internal controls. Thus, the extent of inhibitory innervation on the levator muscle was used to compare to the contralateral unloaded atrophied levator when a cheliped was removed as well as when the limb regenerated. Chelipeds can be induced to autotomize at given periods prior to examining the NMJs. Since regeneration of limbs as an adult for many crustaceans is a normal life process (Morgan, 1900; Zeleny, 1908), the mechanisms of nerve-muscle matching might be accentuated to handle repetitive loading and unloading throughout adult life stages.

The biochemical phenotype of the a.l. muscle was discribed previously (Griffis et al., 2001). The protein profile reveled this muscle to contain both slow and fast fiber types; however, the protein banding profile on SDS-PAGE gels was more similar to slow muscle fiber type than to a purely phasic (fast) muscle types. The mixed profile is expected for the a.l. muscle since mixed muscle type in crustaceans occurs when both tonic and phasic motor nerve innervation is present (Bradacs et al., 1997; Cooper et al., 1998; LaFramboise et al., 2000; Sohn et al., 2000; Griffis et al., 2001; Mykles et al., 2002). The a.l. muscle is mixed in the excitatory innervation (Moffett, 1987; Griffis et al., 2001).

This study is a preliminary investigation into the morphological matching of nerve terminal innervation related to a changing surface area of the a.l. muscle during unloading and reloading due to limb autotomy.

Materials and Methods

Animals and Cheliped Measures

Adult red swamp crayfish, *P. clarkii* (Atchafalaya Biological Supply, Raceland, LA, USA), were used throughout this study. Animals were housed in an aquatic facility and fed dried fish food weekly. Live weights of the intact crayfish were measured, before and after dissection, as were the normal and regenerated limbs (from the autotomy plane forward). An additional measure of cheliped size, the length of the dorsal propus, from the carpus-propus joint to the hinge of the propus-dactylus joint, was measured for each limb (Table 1). The paradigms used in this study for obtaining different degrees of muscle atrophy or regrowth are shown in Fig. 1. The first paradigm includes crayfish with intact chelipeds which serves as a control reference for the other paradigms. The second paradigm is crayfish with one cheliped autotomized without a regenerate appearing at the fracture plane and examine the NMJ after four months. The third paradigm is crayfish with a cheliped that was autotomized but has regenerated. The last paradigm includes both chelipeds autotomized.

Dissection

The dissection techniques used were as outlined in Griffis et al. (2001). In short, the abdomen, the gill chamber, and the walking legs are removed. The remainder of the cephalothorax is cut down the ventral midline. This allowed visualization of the musculature. Dissected preparations were maintained in crayfish saline, a modified Van Harreveld's solution: NaCl (205 mM); KCl (5.3 mM); $CaCl_2 + 2H_2O$ (13.5 mM); $MgCl_2 + 6H_2O$ (2.45 mM); HEPES (0.5 mM) at pH 7.4. Muscles were kept intact until fixation with both the proximal and distal attachments in place with the muscle in a fully stretched position.

Nerve Terminal Visualization

The nerve terminals were visualized by use of the vital stain 4-Di-2-ASP (4-[4-(diethylamino)-styryl]-N-methylpyridinium iodide; Molecular Probes, Eugene, OR, USA) in crayfish saline (Magrassi et al., 1987). This approach

Table 1. Morphometrics in the extant of innervation on the levator muscle. The muscle surface area is the surface area of the muscle bundle that was followed for nerve terminals measured. The area was calculated by length × width of surface facing the viewer. This is a planar surface area, not considering the perimeter of the fiber. TL/SA is the total terminal length per surface area of the muscle bundle. An asterisk indicates the muscle with the greatest degree of atrophy which has the largest ratio of nerve terminal length per surface area of the muscle.

Sample	Muscle length (μm)	Muscle width (μm)	Muscle surface area (μm^2)	Terminal length (μm)	TL/SA ratio ($\times$1000)
Pair with chelipeds (normal)					
Sample 1	6794.8	299.8	2 036 807	3072.2	1.508
Sample 2	9429.15	294.6	2 777 828	3420.42	1.231
One with and one w/o cheliped					
Sample 1 (with)	3467.4	103.4	358 529	754.63	2.105
Sample 2 (w/o)	3152	85.3	268 866	945.23	3.516*
One small and one large					
Sample 1 (small)	4490.23	252.6	1 134 232	3217.54	2.837*
Sample 2 (large)	12 366.91	272.5	3 369 983	2987.9	0.887
Both sides w/o chelipeds					
Sample 1	3788.66	166.8	631 948.5	1947.40	3.082*
Sample 2	4159.53	92.3	383 924.6	1301.67	3.390*

Fig. 1. The types of crayfish used in this study. A, crayfish with intact chelipeds; B, autotomized one cheliped without a regenerate; C, autotomized one cheliped with a regenerate; and D, ones with both chelipeds autotomized.

stained all the terminals (excitatory and inhibitory). Following a wash with fresh saline, nerve terminals were visualized and photographed with a Nikon epifluorescence microscope using a 40× water immersion lens.

Immunocytochemistry

For examining the inhibitory nerve terminals with anti-GABA antibodies the muscles were fixed with 2.5% (v/v) glutaraldehyde, 0.5% (v/v) formaldehyde dissolved in a PBS (phosphate buffer solution) for 1 hr with two changes of solution at room temperature. The PBS solution consisted of 9.5 ml 0.2 M $NaH_2PO_4 \cdot 2H_2O$, 40.5 ml 0.2 M stock $Na_2HPO_4 \cdot 7H_2O$ and 4 g sucrose, brought to 100 ml with H_2O. The muscles were placed into vials and washed in PBS buffer containing 0.5% (v/v) Triton X-100 and 1% (v/v) normal goat serum (Gibco/BRL, Grand Island, NY, USA) with three changes of solution at room temperature for 1 hour. The muscles were then incubated with the primary antibody to GABA (Sigma, 1:1000 in PBS buffer) on a shaker at room temperature for 12 hours followed by three washes in PBS. The muscles were then incubated with secondary antibody (goat, anti-rabbit IgG conjugated with Texas Red, Sigma), diluted 1:200 in PBS, at room temperature for 2 hours. The muscles were washed twice with PBS and mounted in antifade mounting media.

The nerve terminals and muscles were observed with a Leica DM IRBE inverted fluorescent microscope with appropriate illumination. The composite images of Z-series were collected with a Leica TCS NT confocal microscope for illustration and quantifying morphological parameters.

Analysis of Terminals

J-Image software was downloaded from the National Institute of Health (USA) and used for tracing the terminals. The scale bar on the image was first traced for an internal calibrations for the software. The various terminals were then traced for their entire length. The muscle bundle used for the analysis was the longest and most distal bundle in each preparation. This was to standardize the location of the fibers used for comparative purposes. The muscle bundle was also measured for its width and length in order to calculate surface area that was innervated.

Transmission Electron Microscopy (TEM)

All preparations were fixed in a 2.5% gluteraldehyde, 0.5% formaldehyde buffered solution (0.1 M sodium cacodylate, 0.022 wt% $CaCl_2$, 4 wt% sucrose, and adjusted to pH 7.4) for one hour with two changes and post fixed with a 2% osmium tetroxide buffered solution and embedded in Eponate 812. The samples were serially thin sectioned on a Reichert ultracut microtome and post stained with uranyl acetate and lead citrate. Sections were then viewed on a FEI: Philips Tecnai, Bio Twin 12 model transmission electron microscope at 80 kV.

RESULTS

Muscle Atrophy When Unloaded

Levator muscles taken from a crayfish that had one or both chelipeds removed four months earlier showed a dramatic reduction in size and thickness of the muscle bundle on the side with the removed cheliped. Difference where one side had a cheliped removed and the other side was left intact, the comparison in muscle morphology is strikingly different (Fig. 2); the loaded and unloaded muscles both show a whitish color and the same length, but the difference in thickness of the muscle bundles is apparent.

In animals where the muscle was re-loaded by allowing the limb to regenerate, the comparison in muscle mass to controls is not substantially different. Such animals took about six months to grow back a limb the size of the one shown for Fig. 1C. The symmetrical nature of the crayfish allows for comparisons from left and right sides. Crayfish that had both chelipeds removed were able to be compared to ones in which no chelipeds were removed.

After the muscles were dissected out of the animal, they were prepared for various procedures. Some preparations were prepared for transmission electron microscopy (TEM) and others were prepared for immunocytochemical staining to image the extant of neural innervation along the length of the muscle fiber.

Transmission Electron Microscopy

In processing the muscles for TEM the staining procedures turned the muscle black which allowed for good contrast photographs (Fig. 2B). The muscles shown in Fig. 2A are the same as those processed for TEM in Fig. 2B.

The non-atrophied muscle revealed the innervation of multiple terminals and robust muscle fibers (Fig. 3A). Synaptic vesicles along with pre- and post-synaptic thickenings are visualized in higher magnification of the terminals (Fig. 3B). The mitochondria are numerous within the terminal. The motor nerves innervating a atrophied a.l. muscle, from a cheliped removed 4 months earlier, contain mitochondria around the periphery of the axon and a cytoplasm matrix as commonly observed in crayfish motor axons (Bradacs et al., 1997) (Fig. 4A). The skeletal muscle after 4 months of unloading is drastically reduced in size due to the atrophied muscle fibers (Fig. 4B). These atrophied muscles appear to have lost the mass within the muscle fibrils with dense structures that appear to be myosin with the loss of the surrounding actin. This is also a phenomena that appears in human muscle with unloading due to spaceflight with more loss of actin than myosin with muscle atrophy (Fitts et al., 2010). The nerve terminals are reduced in size and contain few mitochondria (Fig. 4C). Vesicles are still observed within the terminals which appear to be present in clusters but synapses are not observed as readily in serial thin sections. The subsynaptic reticulum contains numerous spaces not observed in muscles that remain loaded (Fig. 4D).

Immunocytochemistry: Anti-GABA

The ability to stain selectively one axon and its terminals on the muscle allows one to quantify a single neuron's innervation profile on the muscle with the various experimental

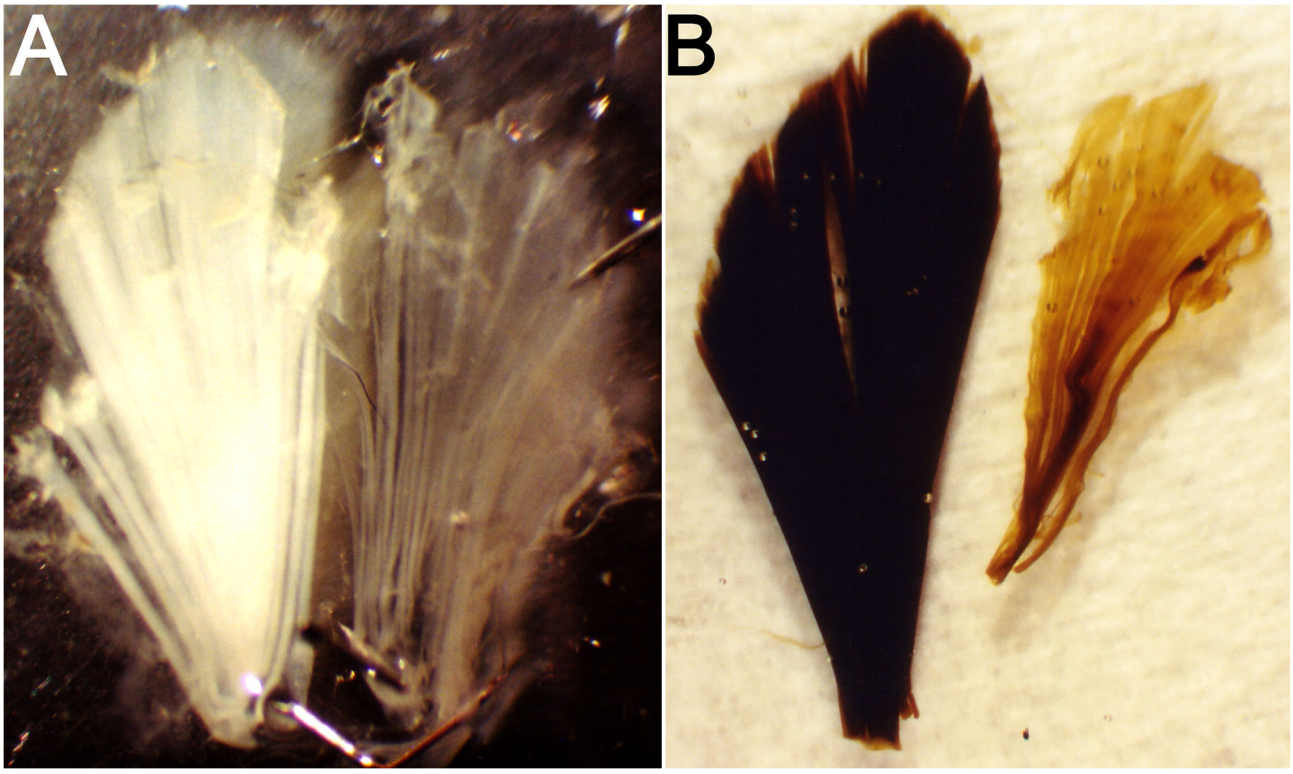

Fig. 2. A, levator muscles from a crayfish with one normal sized cheliped (left) and one that was autotomized 4 months earlier (right). Note the massive muscle atrophy when it was unloaded. B, same muscles shown in left (A) panel but processed for electron microscopy to examine nerve terminals.

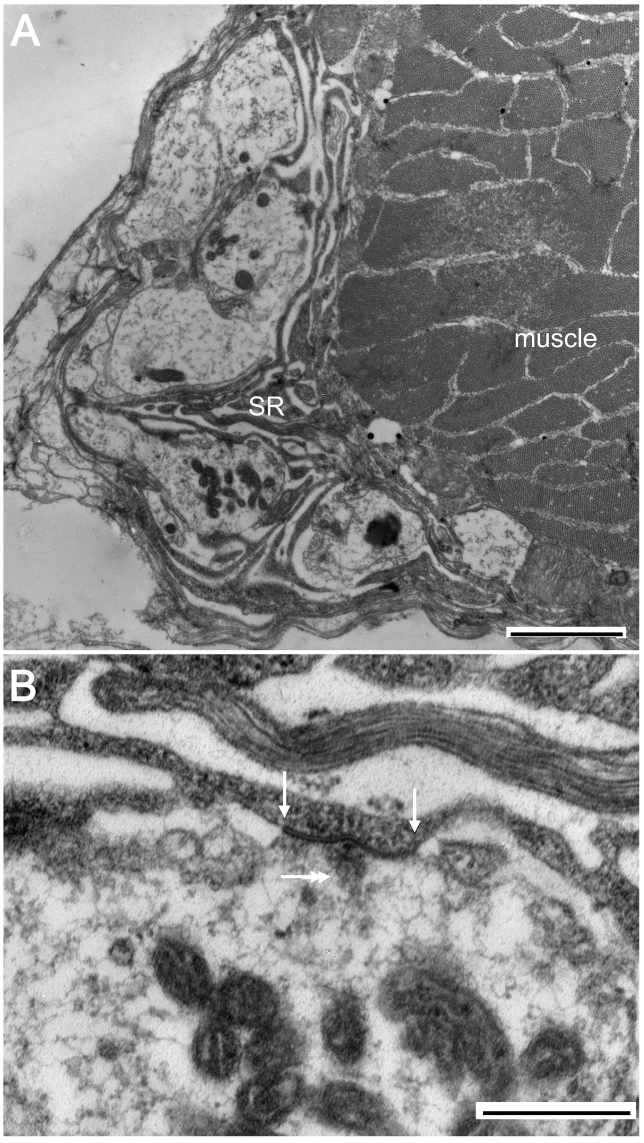

Fig. 3. Innervation of the motor neuron on loaded a.l. muscles. A, multiple terminals and robust muscle fibers are readily observed; B, enlarged view of panel A, which illustrates the synaptic vesicles (double arrow head) within the presynaptic terminal, pre- and post-synaptic thickenings are visualized demarking the synapse (white arrows); C, SR-subsynaptic reticulum. Scale bars (black bar within white): A, 2 μm; B, 500 nm.

paradigms. The opener muscle of the crayfish walking leg was used as a control for anti-GABA immunocytochemistry since only one of the two axons is known to contain GABA (Fig. 5A). Two neurons (excitatory and inhibitory) and their terminals are readily seen when staining the live preparation with 4-Di-2ASP (Fig. 5B).

Representative preparations are shown in Fig. 6A1, B1 for a normal loaded muscle and one that was unloaded that had the cheliped removed four months earlier. The black line on the edges of the muscle bundles show the boarder of the bundle and the red lines depict the various terminals of the inhibitor axon for the loaded and unloaded muscle (Fig. 6A2, B2). To better illustrate the measures used (Fig. 6A3, B3), we show only the traced lines without the muscle.

Measurements

The measurements associated with the nerve terminals and muscle morphology is shown in Table 1 in each of the four experimental paradigms. The ratio of the nerve terminal length to dorsal muscle surface area is the most useful for comparison as this measure standardizes the differences among different size crayfish. The muscle with the greatest degree of atrophy has the largest ratio of nerve terminal length per surface area of the muscle. These particular muscles are indicated with an asterisk ($*$) in Table 1.

When taking these measures of nerve terminal length, we noticed the appearance is different than on control muscles. The nerve terminals on muscles that were atrophied showed many squiggles (Fig. 7). It appears that the muscle mass atrophies at a quicker rate than the nerve terminal being able to regress.

Discussion

In this report we noted that the a.l. muscle will atrophy when it is unloaded and regain its mass upon loading. We also note that the inhibitory nerve on this muscle can readily be identified by a mouse anti-GABA antibody which allowed the innervation profile to be quantified. During atrophy the inhibitory nerve terminal gives an appearance of the muscle being hyperinnervated as compared to control muscle when considering per surface area of muscle bundle. The axons and nerve bundles show squiggles on the atrophied muscle likely from the membrane not being able to be internalized fast enough to match the muscle atrophy (Deschenes et al., 2003). The appearance of the nerve terminals is not sufficient for prediction of functional innervation as the terminals on atrophied muscle have few synaptic sites in comparison but do contain vesicles. Perhaps it is more energy saving to allow the nerve terminals to have excess terminal structure on a muscle since it might regain its normal size in a relatively short time. However, the removal of synaptic structure may reduce the extent of transmission to maintain synaptic homeostasis. Similar muscle atrophy exists for unloading of muscle with astronauts in space for short periods of time without appropriate exercise (Kawano, 2004). Also with muscle disuse, the nerve terminals may alter their functional state while appearing to be unchanged in the general extent of innervation. Thus, ultrastructure needs to be confirmed for a finer resolution of potential synaptic changes.

The TEM serial sections of the nerve terminals on normal and atrophied muscle indicated synaptic vesicles within the terminals on the atrophied muscle but terminals are smaller in diameter and synapses are not as common. This would imply that the terminals are not as high in synaptic efficacy when active. The smaller diameter terminals could add extra membrane that might have otherwise appeared as vesicles or add to the length of the terminal. This could potentially be responsible in part for the squiggles in the long terminals on atrophied muscle.

Perhaps by using the dye FM1-43, which is taken up in vesicles during recycling for all terminals, one could make comparisons if atrophied NMJs showed less staining which would mean fewer vesicles were recycling. This approach might be the most straight forward approach to address the physiological differences of the NMJs for normal and

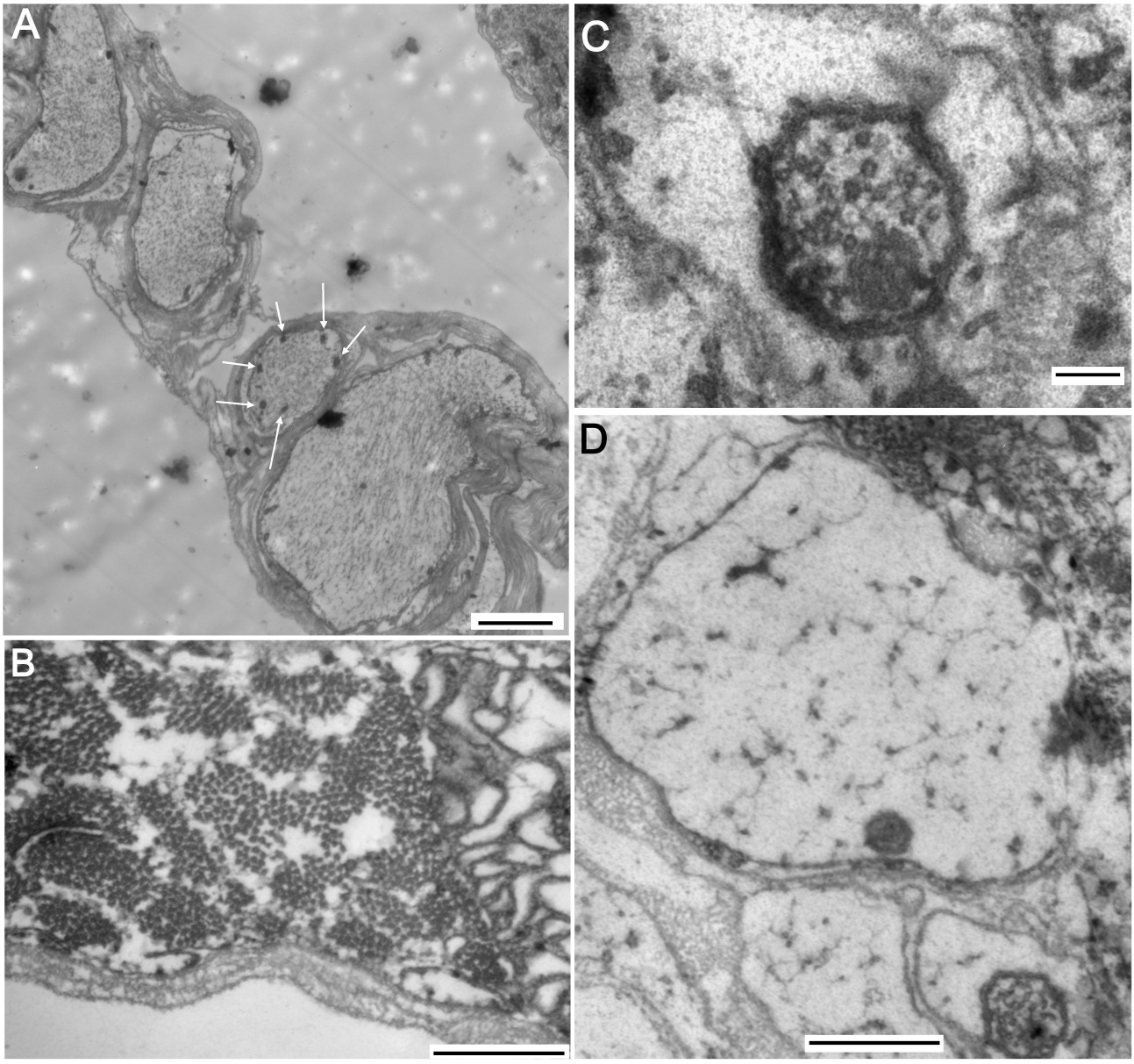

Fig. 4. The morphology on the motor unit on unloaded muscle. A, axons of motor nerves appear normal with a robust cytoplasmic matrix and mitochondria (arrows mark mitochondria for a single axon); B, unloaded muscle exhibits extensive muscle fiber atrophy; C, terminals on the unloaded and atrophied muscles appear small although still contain vesicles, but few synapses; D, there are large gaps present within the subsynaptic reticulum in the atrophied muscles. Scale bars: A, 2 μm; B, 500 nm; C, 100 nm; D, 500 nm.

atrophied muscles. Various questions remain to be addressed in this system: Is it the lack of neural activity that causes the change? Is there a retrograde message from the muscle to the nerve that results in the synaptic regression? Retrograde signals at the frog, mouse, and *Drosophila* are known to alter presynaptic nerve terminals (Herrera and Grinnell, 1980; Grinnell, 1995; Herrera and Zeng, 2003; Bogdanik et al., 2004).

Such potential signals likely exists at crustacean NMJs but the molecular nature of them have not yet been identified. As a future study it would be of interest to identify the anterograde and retrograde signals at NMJs in crustaceans that allow these dynamic changes to occur as well as maintain stable synaptic homeostasis. There are many species of crustaceans that have unique features in motor units (Atwood and Cooper, 1996) which may provide a wide range of possibilities for addressing if commonalities exists or if specialized mechanisms are present. There are still basic phenomenological experiments that need to be conducted which can help to develop experimental paradigms to use in order to target molecular studies. If the a.l. muscle could remain loaded but with a cheliped removed, this would address if it is load alone or if the loss of sensory inputs which dampen the motor drive resulting in muscle atrophy. One might be able to add weights to the limb stump to maintain a load to the a.l. muscle or even accentuate an increase in load to a limb left intact which may lead to hypertrophied muscle. A tendonectomy will unload the muscle with maintaining

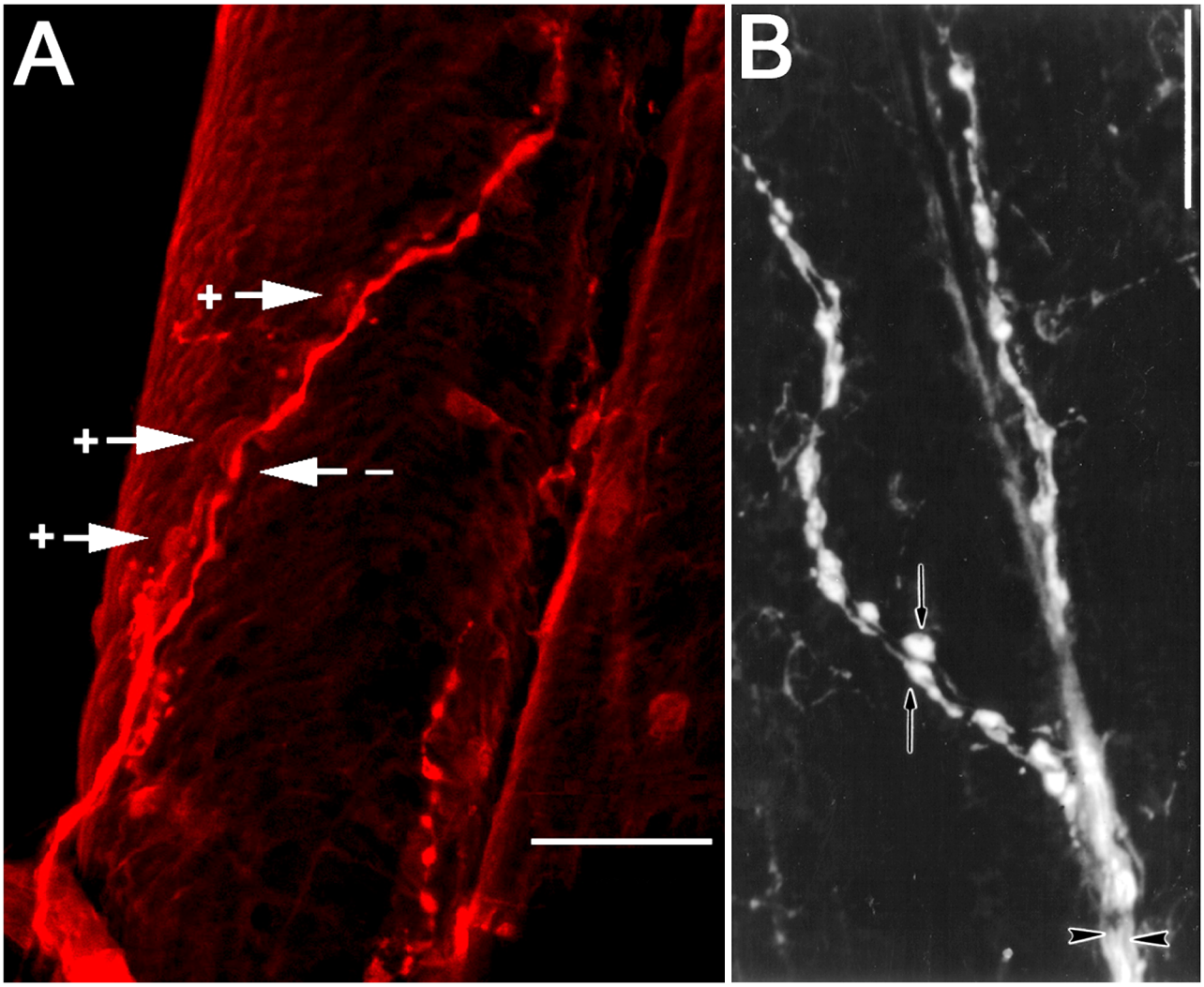

Fig. 5. A, testing anti-GABA antibody staining on opener muscle; B, there are only 2 terminals on the opener – 1 excitor and 1 inhibitor stained with 4-Di-2 ASP. Anti-GABA only binds with 1 terminal on the opener muscle (A). Scale bars: 40 μm; B, 25 μm.

the sensory input to the motor units within the CNS. Perhaps the nerve terminals would regress faster since the muscles would not be able to generate any substantial tension not even passive tension (Velez et al., 1981). Such future manipulations in crustacean preparations will allow one to address mechanisms in muscle to nerve and vice versa while making use of relatively simple preparations in regards to the innervation profile and accessibility.

The cellular mechanisms of muscle atrophy and growth with disuse, unloading, loading and activity is an area of active interest (Siu, 2009; Sudo and Kano, 2009; Chae et al., 2011). The unique nature of skeletal muscle is the fact that it is multinucleated and the reduction or increase in mass that can occur does so in a manner that still allows muscle to function during the transformation (Dupont-Versteegden, 2005; Quadrilatero et al., 2011). What signals the a.l. muscle, used in this present study, to atrophy or grow is unkown. There are known satellite cells present on the surface of skeletal muscle in crayfish (Harrington and Atwood, 1995). They have not been observed under the external lamina by the staining method used for *Procambarus clarkii* (Harrington and Atwood, 1995). However, Novotova and Uhrik (1992), in a different species of crayfish, observed some satellite cells potentially within the muscle cell. It remains to be determined if these satellite cells observed in crayfish are dormant myoblasts that can be used during muscle hypertrophy or regeneration. Recently it was clearly demonstrated in mice that satellite cells on mucsle are not necessary for muscle fiber hypertrophy (McCarthy et al., 2011), but they maybe used for forming new fibers and fiber regeneration. With relatively large muscle fibers, the dynamic nature in atrophy and growth as well as regeneration of limb skeletal muscle in adults, the crustaceans may prove to be a useful model to investigate the interdigitation process of thin and thick filaments during these changes. This cellular process in growth of actively contracting muscle is still an unsolved phenomenon but head way is being made by use of genetic and mutational studies in *Drosophila melanogaster* (Rui et al., 2010).

The NMJs in invertebrates serve as usefull models for investigating synaptic homeostasis due to their graded responses and requirment for tight matching in muscle depo-

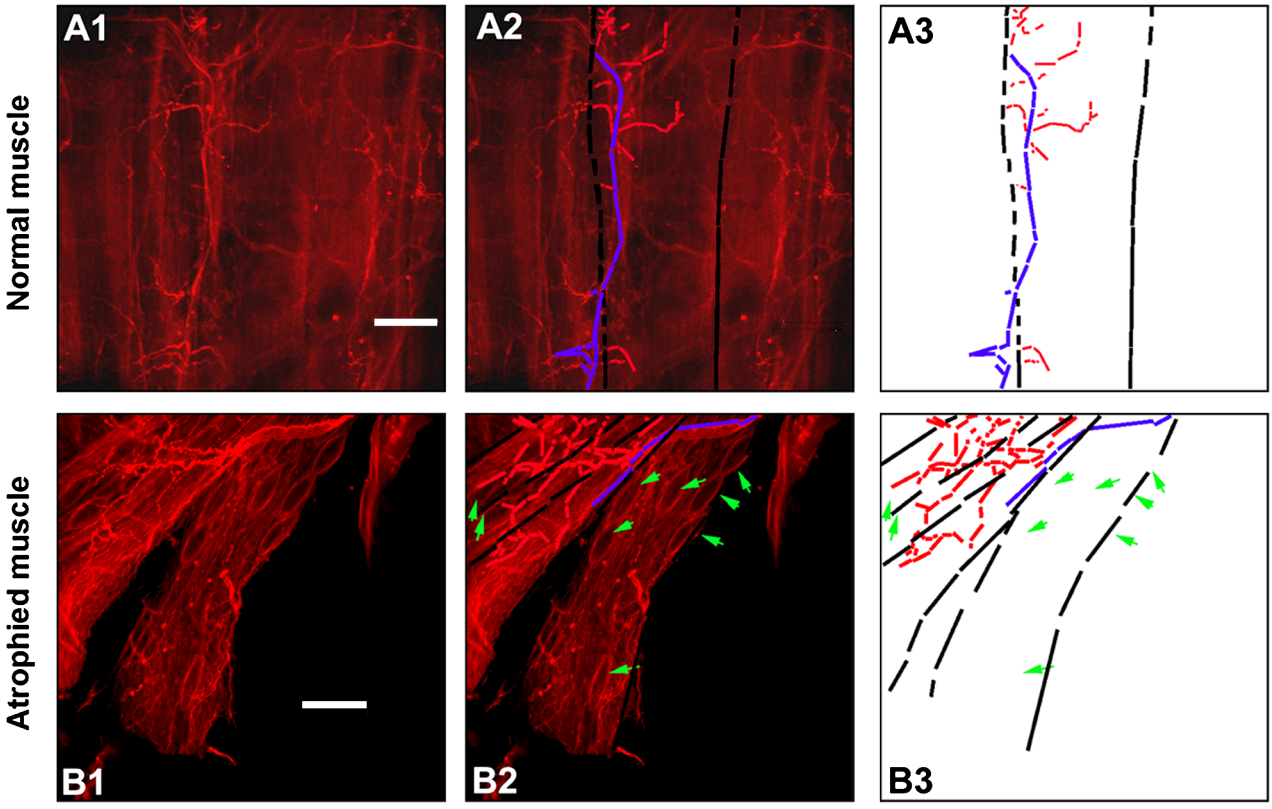

Fig. 6. Levator muscles stained with anti-GABA in loaded (top A panels) and unloaded (bottom B panels) muscles. Black lines outline muscle bundles (A2 and B2). Blue lines axon preterminal, red lines the terminals with varicosities. Green arrows show parasitic cysts in the muscle. These cysts are very prevalent in atrophied muscle. The traced terminals are shown in A3 and B3 which are used for measured values. Scale bars: A1 and B1, 40 μm.

larization and force generation. The forward and retrograde signaling mechanisms for homestatic regulation of synaptic function in general is still being tackled and many of the cellular processes are being identified at NMJs. The advantages in genetic manipulations of *Drosophila melanogaster* have opened many avenues into the pre- and post-synaptic regulation of synaptic maintainence and organization during devlopment (Stewart et al., 1996; Li et al., 2002; Xing et al., 2005; Frank, 2006; Henry et al., 2012; Penny et al., 2012). The regulation in complexity of synaptic structure in conjunction of synaptic strength appear to be common among *D. melanogaster* and crayfish (Atwood and Cooper, 1995, 1996a, b; Cooper et al., 1996; Stewart et al., 1996; Johnstone et al., 2011). The postsynaptic glutamate receptors also show similar pharmacological profiles (Lee et al., 2009). As compared to insects, the dynamic intrinsic nature in limb regeneration, atrophy and regrowth with molting may offer additional advantages in mature crustaceans. The large size and rapid growth of muscle in some crustaceans have yet to be tapped for investigation into the molecular mechanisms in synaptic homeostatic regulation. The similarities among the species suggest a default in low metabolic stasis in muscle mass and synaptic transmission, as disuse promotes rapid muscle atrophy, nerve terminal structural and functional degradation in insects and rodents (Kidokoro et al., 2004; Marimuthu et al., 2011; Talbert et al., 2013) as compared to activity promoting growth and synaptic stabilization. How the synapses maintain an organized synaptic efficacy to match muscle needs during regulated growth or atrophy continues to be allusive.

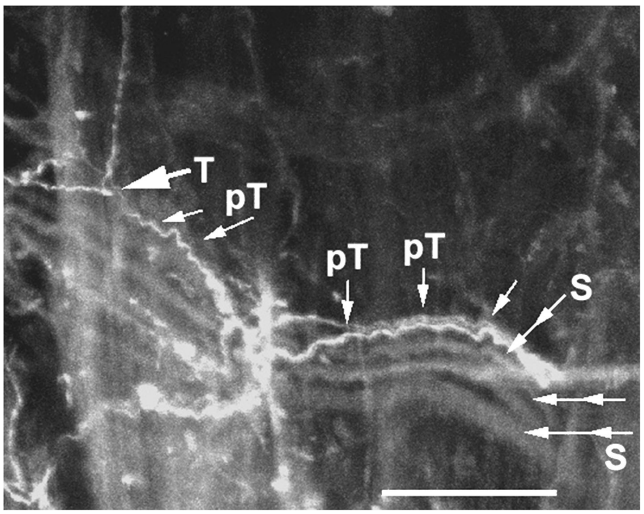

Fig. 7. With muscle atrophy the nerve and nerve terminals are not as stretched and thus show wiggles. Does the nerve reabsorb the nerve membrane over time? T = terminal, pT = preterminal, S = nerve sheath. Scale bar: 100 μm.

Understanding the molecular mechanisms in dynamics of muscle growth and atrophy can help in understanding disease processes for potential therapy in humans (Gielen et al., 2003; Chin, 2005; Dupont-Versteegden, 2005; Tisdale,

2007; French et al., 2008; O'Leary and Hood, 2008; Glass, 2010; Reid and Moylan, 2011). The potential mechanisms to reduce protein synthesis in muscle may in part be due to apoptotic cascades known in other cell types (Li et al., 2001; Parise and De Lisio, 2010). Thus, various cellular responses need to be investigated as the processes may apply to skeletal muscle. In addition, comparative studies in invertebrates does allow ease in experimentation not so readily obtained in mammals and can set a stage for screening various mechanisms that are applicable for mammals (Brand and Livesey, 2011; Pandey and Nichols, 2011; MacLea et al., 2012; Neckameyer and Argue, 2013).

ACKNOWLEDGEMENTS

This work was funded in part by Kentucky Young Researchers, University of Kentucky (ASC) and personal funds (RLC).

REFERENCES

Atwood, H. L. 1973. An attempt to account for the diversity of crustacean muscles. American Zoologist 13: 357-378.

———, and R. L. Cooper. 1995. Functional and structural parallels in crustaceans and *Drosophila* neuromuscular systems. American Zoologist 35: 556-565.

———, and ———. 1996. Assessing ultrastructure of crustacean and insect neuromuscular junctions. Journal of Neuroscience Methods 69: 51-58.

———, and ———. 1996. Synaptic diversity and differentiation: crustacean neuromuscular junctions. Invertebrate Neuroscience 1: 291-307.

Balice-Gordon, R. J., S. M. Breedlove, S. Bernstein, and J. W. Lightman. 1990. Neuromuscular junctions shrink and expand as muscle fiber size is manipulated: in vitro observation in the androgen-sensitive bulbocavernosus muscle of mice. Journal of Neuroscience 10: 2660-2671.

Bradacs, H., R. L. Cooper, M. Msghina, and H. L. Atwood. 1997. Differential physiology and morphology of phasic and tonic motor axons in a crayfish limb extensor muscle. Journal Experimental Biology 200: 677-691.

Brand, A. H., and F. J. Livesey. 2011. Neural stem cell biology in vertebrates and invertebrates: more alike than different? Neuron 70: 719-729.

Bogdanik, L., R. Mohrmann, A. Ramaekers, J. Bockaert, Y. Grau, K. Broadie, and M. L. Parmentier. 2004. The *Drosophila* metabotropic glutamate receptor DmGluRA regulates activity-dependent synaptic facilitation and fine synaptic morphology. Journal of Neuroscience 24: 9105-9116.

Chae, C. H., S. L. Jung, S. H. An, C. K. Jung, S. N. Nam, and H. T. Kim. 2011. Treadmill exercise suppresses muscle cell apoptosis by increasing nerve growth factor levels and stimulating p-phosphatidylinositol 3-kinase activation in the soleus of diabetic rats. Journal of Physiological Biochemistry 67: 235-241.

Chin, E. R. 2005. Role of Ca^{2+}/calmodulin-dependent kinases in skeletal muscle plasticity. Journal of Applied Physiology 99: 414-423.

Cooper, A. S., and R. L. Cooper. 2009. Historical view and demonstration of physiology at the NMJ at the crayfish opener muscle. Journal of Visualized Experiments 33: available online at http://www.jove.com/index/details.stp?id=1595, DOI:10.3791/1595.

Cooper, R. L., C. Harrington, L. Marin, and H. L. Atwood. 1996. Quantal release at visualized terminals of crayfish motor axon: intraterminal and regional differences. Journal of Comparative Neurology 375: 583-600.

———, L. Marin, and H. L. Atwood. 1995. Synaptic differentiation of a single motor neuron: conjoint definition of transmitter release, presynaptic calcium signals and ultrastructure. Journal of Neuroscience 15: 4209-4222.

———, W. M. Warren, and H. E. Ashby. 1998. Activity of phasic motor neurons partially transforms the neuronal and muscle phenotype to a tonic-like state. Muscle Nerve 21: 921-931.

Del Castillo, J., and B. Katz. 1954. Quantal components of the end-plate potential. Journal of Physiology 124: 560-573.

Deschenes, M. R., K. M. Will, F. W. Booth, and S. E. Gordon. 2003. Unlike myofibers, neuromuscular junctions remain stable during prolonged muscle unloading. Journal of Neurology Science 210: 5-10.

Dupont-Versteegden, E. E. 2005. Apoptosis in muscle atrophy: relevance to sarcopenia. Experimental Gerontology 40: 473-481.

Edgerton, V. R., and R. R. Roy. 1994. Neuromuscular adaptation to actual and simulated weightlessness. Advance Space Biological Medicine 4: 33-67.

Fatt, P., and B. Katz. 1953a. The electrical properties of crustacean muscle fibers. Journal of Physiology 120: 171-204.

———, and ———. 1953b. Distributed 'endplate potentials' of crustacean muscle fibres. Journal of Experimental Biology 30: 433-439.

Fitts, R. H., S. W. Trappe, D. L. Costill, P. M. Gallagher, A. C. Creer, P. A. Colloton, J. R. Peters, J. G. Romatowski, J. L. Bain, and D. A. Riley. 2010. Prolonged space flight-induced alterations in the structure and function of human skeletal muscle fibres. Journal of Physiology 588: 3567-3592.

Frank, C. A., M. J. Kennedy, C. P. Goold, K. W. Marek, and G. W. Davis. 2006. Mechanisms underlying the rapid induction and sustained expression of synaptic homeostasis. Neuron 52: 663-677.

French, J. P., K. L. Hamilton, J. C. Quindry, Y. Lee, P. A. Upchurch, and S. K. Powers. 2008. Exercise-induced protection against myocardial apoptosis and necrosis: MnSOD, calcium-handling proteins, and calpain. FASEB Journal 22: 2862-2871.

Gielen, S., V. Adams, S. Mobius-Winkler, A. Linke, S. Erbs, J. Yu, W. Kempf, A. Schubert, G. Schuler, and R. Hambrecht. 2003. Anti-inflammatory effects of exercise training in the skeletal muscle of patients with chronic heart failure. Journal of American College of Cardiology 42: 861-868.

Girard, C. 1852. A revision of the North American astaci, with observations on their habits and geographic distribution. Proceedings of the Academy of Natural Sciences of Philadelphia 6: 87-91.

Glass, D. J. 2010. PI3 kinase regulation of skeletal muscle hypertrophy and atrophy. Current Topics in Microbiology and Immunology 346: 267-278.

Goldstein, A., P. Bhatia, and J. M. Vento. 2012. Update on nuclear mitochondrial genes and neurologic disorders. Seminars in Pediatric Neurology 19: 181-193.

Griffis, B., S. Moffett, and R. L. Cooper. 2001. Muscle phentype remains unaltered after limb autotomy and unloading. Journal of Experimental Zoology 289: 10-22.

Grinnell, A. D. 1995. Dynamics of nerve-muscle interaction in developing and mature neuromuscular junctions. Physiological Reviews 75: 789-834.

Harrington, C. C., and H. L. Atwood. 1995. "Satellite cells" and nerve terminals in the crayfish opener muscle visualized with fluorescent dyes. Journal of Comparative Neurology 361: 441-450.

Henry, F. E., A. J. McCartney, R. Neely, A. S. Perez, C. J. Carruthers, E. L. Stuenkel, K. Inoki, and M. A. Sutton. 2012. Retrograde changes in presynaptic function driven by dendritic mTORC1. Journal of Neuroscience 32: 17128-17142.

Herrera, A. A., and A. D. Grinnell. 1980. Transmitter release from frog motor nerve terminals depends on motor unit size. Nature 287: 649-651.

———, and Y. Zeng. 2003. Activity-dependent switch from synapse formation to synapse elimination during development of neuromuscular junctions. Journal of Neurocytology 32: 817-833.

Hubel, D. H., and T. N. Wiesel. 1970. The period of susceptibility to the physiological effects of unilateral eye closure in kittens. Journal of Physiology 206: 419-436.

Johnstone, A. F. M., K. Viele, and R. L. Cooper. 2011. Structure/function assessment of crayfish neuromuscular junctions. Synapse 65: 287-299.

Kawano, F. 2004. The mechanisms underlying neuromuscular changes in microgravity environment. Biological Sciences in Space 18: 104-105.

Kidokoro, Y., H. Kuromi, R. Delgado, C. Maureira, C. Oliva, and P. Labarca. 2004. Synaptic vesicle pools and plasticity of synaptic transmission at the *Drosophila* synapse. Brain Research Reviews 47: 18-32.

LaFramboise, W. A., B. Griffis, P. Bonner, W. Warren, D. Scalise, R. D. Guthrie, and R. L. Cooper. 2000. Muscle type-specific myosin isoforms in crustacean muscles. Journal of Experimental Zoology 286: 36-48.

Lee, J.-Y., D. Bhatt, D. Bhatt, W.-Y. Chung, and R. L. Cooper. 2009. Furthering pharmacological and physiological assessment of the glutamatergic receptors at the *Drosophila* neuromuscular junction. Comparative Biochemistry and Physiology, Part C 150: 546-557.

Li, H., X. Peng, and R. L. Cooper. 2002. Development of *Drosophila* larval neuromuscular junctions: maintaining synaptic strength. Neuroscience 115: 505-513.

Li, L. Y., X. Luo, and X. Wang. 2001. Endonuclease G is an apoptotic DNase when released from mitochondria. Nature 412: 95-99.

Lomo, T. 2003. What controls the position, number, size, and distribution of neuromuscular junctions on rat muscle fibers? Journal of Neurocytology 32: 835-848.

MacLea, K. S., A. M. Abuhagr, N. L. Pitts, J. A. Covi, B. D. Bader, E. S. Chang, and D. L. Mykles. 2012. Rheb, an activator of target of rapamycin, in the blackback land crab, *Gecarcinus lateralis*: cloning and effects of molting and unweighting on expression in skeletal muscle. Journal of Experimental Biology 215: 590-604.

Magrassi, L., D. Purves, and J. W. Lichtman. 1987. Flourescent probes that stain living nerve terminals. Journal of Neuroscience 7: 1207-1214.

Marimuthu, K., A. J. Murton, and P. L. Greenhaff. 2011. Mechanisms regulating muscle mass during disuse atrophy and rehabilitation in humans. Journal of Applied Physiology 110: 555-560.

Marques, G. 2005. Morphogens and synaptogenesis in *Drosophila*. Journal of Neurobiology 64: 417-434.

McCarthy, J. J., J. Mula, M. Miyazaki, R. Erfani, K. Garrison, A. B. Farooqui, R. Srikuea, B. A. Lawson, B. Grimes, C. Keller, G. Van Zant, K. S. Campbell, K. A. Esser, E. E. Dupont-Versteegden, and C. A. Peterson. 2011. Effective fiber hypertrophy in satellite cell-depleted skeletal muscle. Development 138: 3657-3666.

Moffett, S. B. 1987. Muscles proximal to the fracture plane atrophy after limb autotomy in decapod crustaceans. Journal of Experimental Zoology 244: 485-490.

Morgan, T. H. 1900. Further experiments on regeneration in Crustacea. Journal of Experimental Biology 21: 144-146.

Mykles, D. L., S. A. Medler, A. Koenders, and R. L. Cooper. 2002. Myofibrillar protein isoform expression is correlated with synaptic efficacy in slow fibres of the claw and leg opener muscles of crayfish and lobster. Journal of Experimental Biology 205: 513-522.

Neckameyer, W. S., and K. J. Argue. 2012. Comparative approaches to the study of physiology: *Drosophila* as a physiological tool. American Journal of Physiology. Regulatory, Integrative Comparative Physiology 304: R177-R188.

Novotová, M., and B. Uhrík. 1992. Structural characteristics and distribution of satellite cells along crayfish muscle fibers. Experientia 48: 593-596.

Ohira, Y. 2000. Neuromuscular adaptation to microgravity environment. Japan Journal of Physiology 50: 303-314.

O'Leary, M. F., and D. A. Hood. 2008. Effect of prior chronic contractile activity on mitochondrial function and apoptotic protein expression in denervated muscle. Journal of Applied Physiology 105: 114-120.

Owen, J. P., Y. O. Li, E. Ziv, Z. Strominger, J. Gold, P. Bukhpun, M. Wakahiro, E. J. Friedman, E. H. Sherr, and P. Mukherjee. 2012. The structural connectome of the human brain in agenesis of the corpus callosum. Neuroimage 70: 340-355.

Pacifici, P. G., C. Peter, P. Yampolsky, M. Koenen, J. J. McArdle, and V. Witzemann. 2011. Novel mouse model reveals distinct activity-dependent and -independent contributions to synapse development. PLoS One 6(1): e16469, DOI:10.1371/journal.pone.0016469.

Pandey, U. B., and C. D. Nichols. 2011. Human disease models in *Drosophila melanogaster* and the role of the fly in therapeutic drug discovery. Pharmacology Reviews 63: 411-436.

Parise, G., and M. De Lisio. 2010. Mitochondrial theory of aging in human age-related sarcopenia. Interdiscipinary Topics in Gerontology 37: 142-156.

Penney, J., K. Tsurudome, E. H. Liao, F. Elazzouzi, M. Livingstone, M. Gonzalez, N. Sonenberg, and A. P. Haghighi. 2012. TOR is required for the retrograde regulation of synaptic homeostasis at the *Drosophila* neuromuscular junction. Neuron 74: 166-178.

Quadrilatero, J., S. E. Alway, and E. E. Dupont-Versteegden. 2011. Skeletal muscle apoptotic response to physical activity: potential mechanisms for protection. Applied Physiology, Nutrition and Metabolism 36: 608-617.

Reid, M. B. 2001. Invited review: Redox modulation of skeletal muscle contraction: what we know and what we don't. Journal of Applied Physiology 90: 724-731.

———. 2005. Response of the ubiquitin-proteasome pathway to changes in muscle activity. American Journal of Physiology. Regulatory, Integrative Comparative Physiology 288: 1423-1431.

———, and J. S. Moylan. 2011. Beyond atrophy: redox mechanisms of muscle dysfunction in chronic inflammatory disease. Journal of Physiology 589: 2171-2179.

Rui, Y., J. Bai, and N. Perrimon. 2010. Sarcomere formation occurs by the assembly of multiple latent protein complexes. PLoS Genetics 6(11): e1001208, DOI:10.1371/journal.pgen.1001208.

Sanes, J. R., and J. W. Lichtman. 1999. Development of the vertebrate neuromuscular junction. Annual Reviews in Neuroscience 22: 389-442.

Siu, P. M. 2009. Muscle apoptotic response to denervation, disuse, and aging. Medicine and Science in Sports Exercise 41: 1876-1886.

Sohn, J., D. L. Mykles, and R. L. Cooper. 2000. The anatomical, physiological and biochemical characterization of muscles associated with the articulating membrane in the dorsal surface of the crayfish abdomen. Journal of Experimental Zoology 287: 353-377.

Stewart, B. A., C. M. Schuster, C. S. Goodman, and H. L. Atwood. 1996. Homeostasis of synaptic transmission in *Drosophila* with genetically altered nerve terminal morphology. Journal of Neuroscience 16: 3877-3886.

Sudo, M., and Y. Kano. 2009. Myofiber apoptosis occurs in the inflammation and regeneration phase following eccentric contractions in rats. Journal of Physiological Science 59: 405-412.

Talbert, E. E., A. J. Smuder, K. Min, O. S. Kwon, and S. K. Powers. 2013. Calpain and caspase-3 play required roles in immobilization-induced limb muscle atrophy. Journal of Applied Physiology 114: 1482-1489.

Talmadge, R. J. 2000. Myosin heavy chain isoform expression following reduced neuromuscular activity: potential regulatory mechanisms. Muscle Nerve 23: 661-679.

Tisdale, M. J. 2007. Is there a common mechanism linking muscle wasting in various disease types? Current Opinion in Supportive Palliative Care 1: 287-292.

Turner, M. B., T. M. Szabo-Maas, J. C. Poyer, and M. J. Zoran. 2011. Regulation and restoration of motoneuronal synaptic transmission during neuromuscular regeneration in the pulmonate snail *Helisoma trivolvis*. Biological Bulletin 221: 110-125.

Velez, S. J., G. D. Bittner, H. L. Atwood, and C. K. Govind. 1981. Trophic interactions of crayfish muscle fibers and neuromuscular synapses after denervation, tenotomy and immobilization. Experimental Neurology 71: 307-325.

Xing, B., A. A. Long, D. A. Harrison, and R. L. Cooper. 2005. Developmental consequences of NMJs with reduced presynaptic calcium channel function. Synapse 57: 132-147.

Zeleny, C. 1908. Some internal factors concerned with the regeneration of the chelae of the gulf-weed rab (*Portunus sayi*). Papers from the Tortugas Laboratory, Carnegie Institute of WA 2: 103-138.

RECEIVED: 23 May 2013.
ACCEPTED: 9 July 2013.
AVAILABLE ONLINE: 28 August 2013.